

INVENTORY SUPPLEMENTAL MATERIAL

Figures

[Figure S1](#). SR protein poison exons are differentially spliced to regulate SR protein expression during iPSC differentiation and in tumors

[Figure S2](#). Splicing of SR protein poison exons is regulated by multiple RBPs

[Figure S3](#). SR protein poison exon sequences contain binding sites for their other protein family members

[Figure S4](#). SR proteins use poison exons to auto- and cross-regulate their protein expression

[Figure S5](#). SR proteins cross-regulate their expression in a dose-dependent manner through alternative splicing of poison exons

[Figure S6](#). Defining the splicing regulatory elements and splicing regulators of *TRA2 β -PE* inclusion

[Figure S7](#). TRA2 β -targeting ASOs impact *TRA2 β -PE* splicing as well as TRA2 β protein expression and activity

Tables

[Table S1](#). Computational analysis of differential splicing in human tumor samples

[Table S2](#). Analysis of RBP binding to SR protein poison exon sequences

[Table S3](#). Correlation of SR protein minigene splicing and protein expression

[Table S4](#). Sequence based reagents used in this study

Figure S1

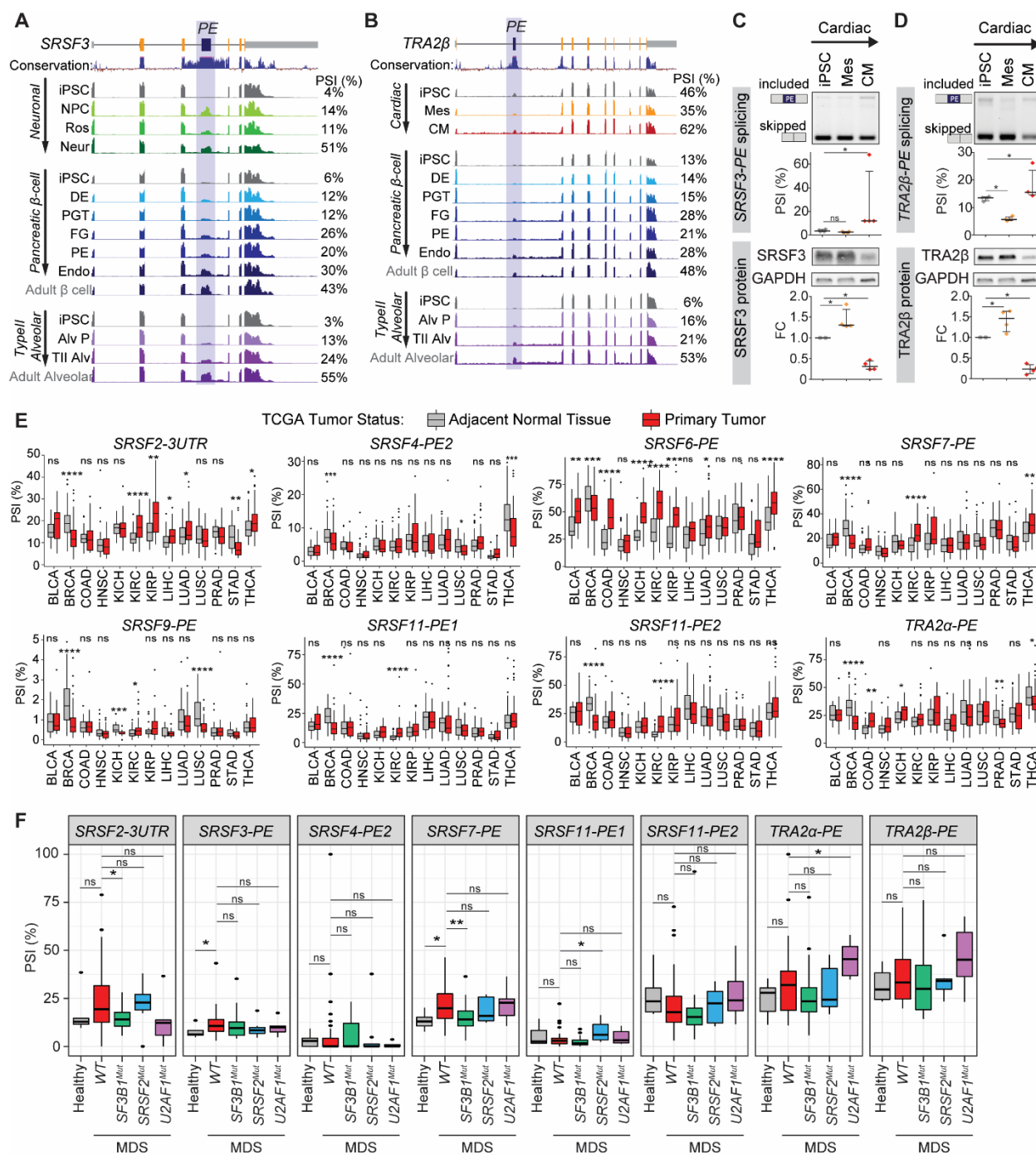


Figure S1. SR protein poison exons are differentially spliced to regulate SR protein expression during iPSC differentiation and in tumors (related to Figure 1).

(A) *SRSF3*-PE inclusion in iPSCs differentiated into neurons, pancreatic β -cells, or Type II alveolar lung epithelial cells visualized using RNA-seq read coverage for the entire gene region. Evolutionary conservation across 100 vertebrates shows the location of ultraconserved regions.

Average exon inclusion (PSI) values from replicates are listed ($n \geq 3$ for all timepoints, except $n=2$ for adult β -cells).

iPSC neuronal ($n=18$); NPC, neural progenitor cells ($n=20$); Ros, neural rosette ($n=13$); Neur, mature neurons ($n=4$); iPSC pancreatic ($n=3$); DE, definitive endoderm ($n=3$); PGT, primitive gut tube ($n=3$); FG, posterior foregut ($n=3$); PE, pancreatic endoderm ($n=3$); Endo, *in vivo* matured endocrine cells ($n=4$); Adult β C, isolated β -cells from adult patients ($n=2$); iPSC alveolar ($n=3$); AlvP, day 15 alveolar epithelial progenitors ($n=3$); AlvTII, day 35 *in vitro* differentiated type II alveolar epithelial cells ($n=3$); AdultTII, isolated type II alveolar cells from adult patients ($n=3$).

(B) Same as in (A) for *TRA2 β -PE* inclusion in iPSCs differentiated into cardiomyocytes, pancreatic β -cells, or Type II alveolar lung epithelial cells.

iPSC cardiac ($n=4$); Mes, Mesoderm ($n=4$); CM, cardiomyocytes ($n=4$); iPSC pancreatic ($n=3$); DE, definitive endoderm ($n=3$); PGT, primitive gut tube ($n=3$); FG, posterior foregut ($n=3$); PE, pancreatic endoderm ($n=3$); Endo, *in vivo* matured endocrine cells ($n=4$); Adult β C, isolated β -cells from adult patients ($n=2$); iPSC alveolar ($n=3$); AlvP, day 15 alveolar epithelial progenitors ($n=3$); AlvTII, day 35 *in vitro* differentiated type II alveolar epithelial cells ($n=3$); AdultTII, isolated type II alveolar cells from adult patients ($n=3$).

(C,D) *SRSF3-PE* (C) or *TRA2 β -PE* (D) inclusion and corresponding protein levels in iPSCs differentiated into mesoderm (Mes) or cardiomyocytes (CM). PE inclusion, quantified as percent spliced in (PSI), is measured by semi-quantitative RT-PCR using primers that amplify both the included and skipped isoforms ($n=4$, median \pm interquartile range; Wilcoxon rank test, $*P < 0.05$). Fold change (FC) protein expression is quantified by western blot using SRSF3 or TRA2 β antibodies and GAPDH as a loading control, normalized iPSCs ($n=4$, median \pm interquartile range; Wilcoxon rank test, $*P < 0.05$).

(E) Inclusion of *SR-PEs*, quantified as percent spliced in (PSI), across TCGA tumor types with ≥ 15 tumor and patient matched adjacent normal tissue samples ($n \geq 30$; Wilcoxon rank test, $*P < 0.05$, $**P < 0.01$, $***P < 0.001$, $****P < 0.0001$, ns - not significant). See also [Table S1](#).

BLCA, Bladder urothelial carcinoma ($n=39$); BRCA, Breast invasive carcinoma ($n=213$); COAD, Colon adenocarcinoma ($n=50$); HNSC, Head and neck squamous cell carcinoma ($n=84$); KICH, Kidney chromophobe ($n=45$); KIRC, kidney renal clear cell carcinoma ($n=132$); KIRP, kidney renal papillary cell carcinoma ($n=52$); LIHC, Liver hepatocellular carcinoma ($n=77$); LUAD, Lung adenocarcinoma ($n=109$); LUSC, Lung squamous cell carcinoma ($n=96$); PRAD, prostate adenocarcinoma ($n=104$); STAD, Stomach adenocarcinoma ($n=50$); THCA, Thyroid carcinoma ($n=116$).

(F) Inclusion of *SR-PEs*, quantified as PSI, in CD34⁺ cells from myelodysplastic syndrome (MDS) patients with SF mutations (*SF3B1*^{Mut} $n=28$, *SRSF2*^{Mut} $n=8$, or *U2AF1*^{Mut} $n=6$), myelodysplastic syndrome patients without SF mutations (*WT*, $n=40$), or healthy controls ($n=8$) (Pellagatti et al., 2018) (Wilcoxon rank test, $*P < 0.05$, $**P < 0.01$, $***P < 0.001$, $****P < 0.0001$, ns - not significant). See also [Table S1](#).

Figure S2

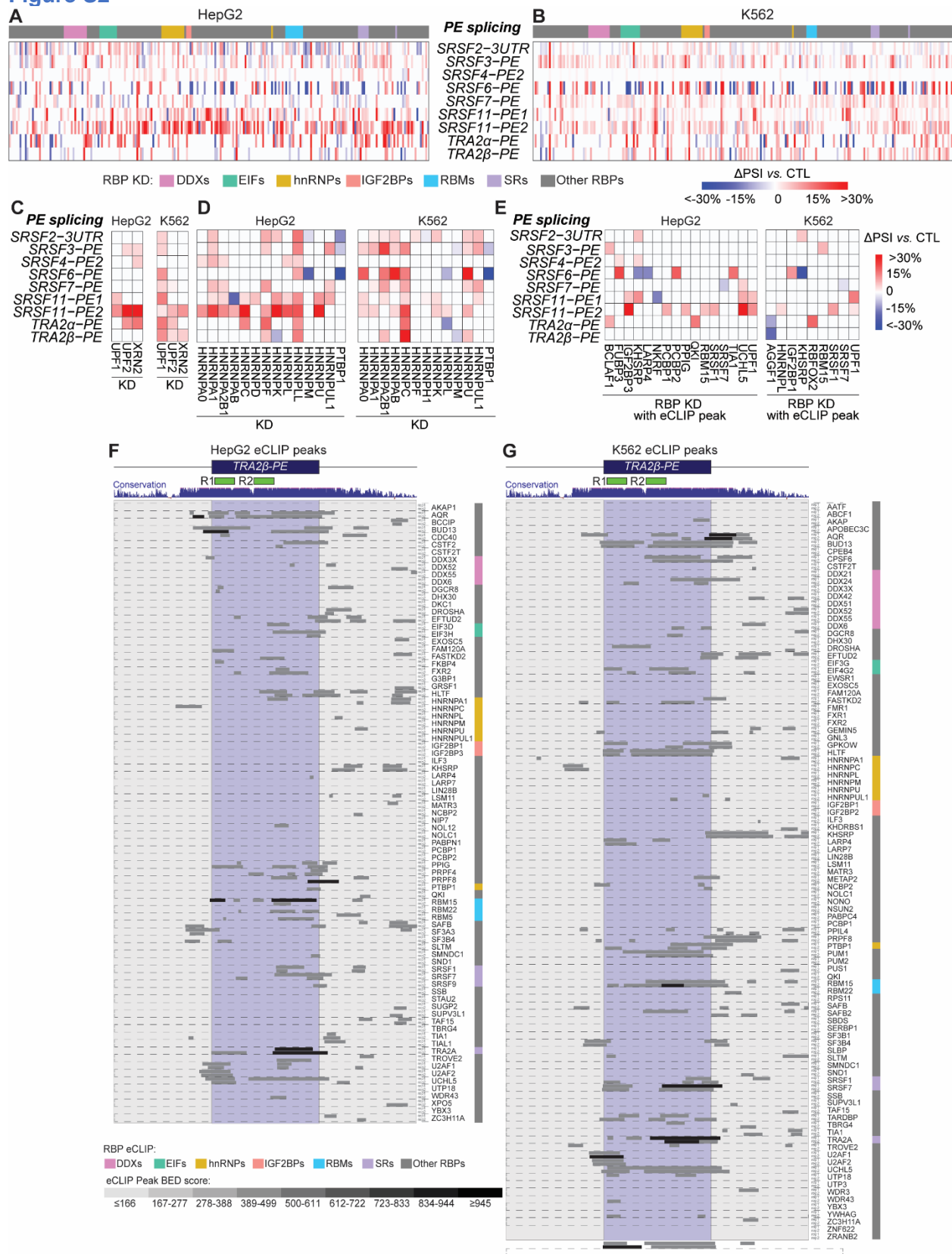


Figure S2. Splicing of SR protein poison exons is regulated by multiple RNA binding proteins (related to Figure 2).

(A,B) *SR-PE* inclusion is quantified as Percent spliced-in (PSI) in HepG2 (**A**) or K562 cells (**B**) with *SR* protein KD (ENCODE). Increased exon inclusion ($\Delta\text{PSI}>0$) or skipping ($\Delta\text{PSI}<0$) is relative to control ($n=2$; rMATS, likelihood ratio $P>0.05$).

(C) *SR-PE* inclusion in HepG2 or K562 cells (ENCODE) with KD of RBPs involved in NMD. Increased exon inclusion ($\Delta\text{PSI}>0$) or skipping ($\Delta\text{PSI}<0$) is relative to control ($n=2$; rMATS, likelihood ratio $P>0.05$).

(D) *SR-PE* inclusion in HepG2 or K562 cells with hnRNP protein KD (ENCODE). Increased exon inclusion ($\Delta\text{PSI}>0$) or skipping ($\Delta\text{PSI}<0$) is relative to control ($n=2$; rMATS, likelihood ratio $P>0.05$).

(E) *SR-PE* inclusion for RBPs that impact splicing in **(A,B)** and bind the *SR* protein ultraconserved regions as evidenced by the presence of RBP eCLIP peaks in HepG2 or K562 cells (ENCODE). Increased exon inclusion ($\Delta\text{PSI}>0$) or skipping ($\Delta\text{PSI}<0$) is relative to control ($n=2$; rMATS, likelihood ratio $P>0.05$).

(F-G) eCLIP binding peaks from individual RBPs in the *TRA2 β -PE* region in HepG2 (**F**) and K562 (**G**) cells (ENCODE). Schematic of *TRA2 β -PE* genomic region, the evolutionary conservation across 100 vertebrates, and the locations of region 1 (R1) and region 2 (R2) from Figure 5C are shown. Scores for eCLIP peaks from ENCODE are indicated; peaks with the strongest support are colored in black.

Figure S3

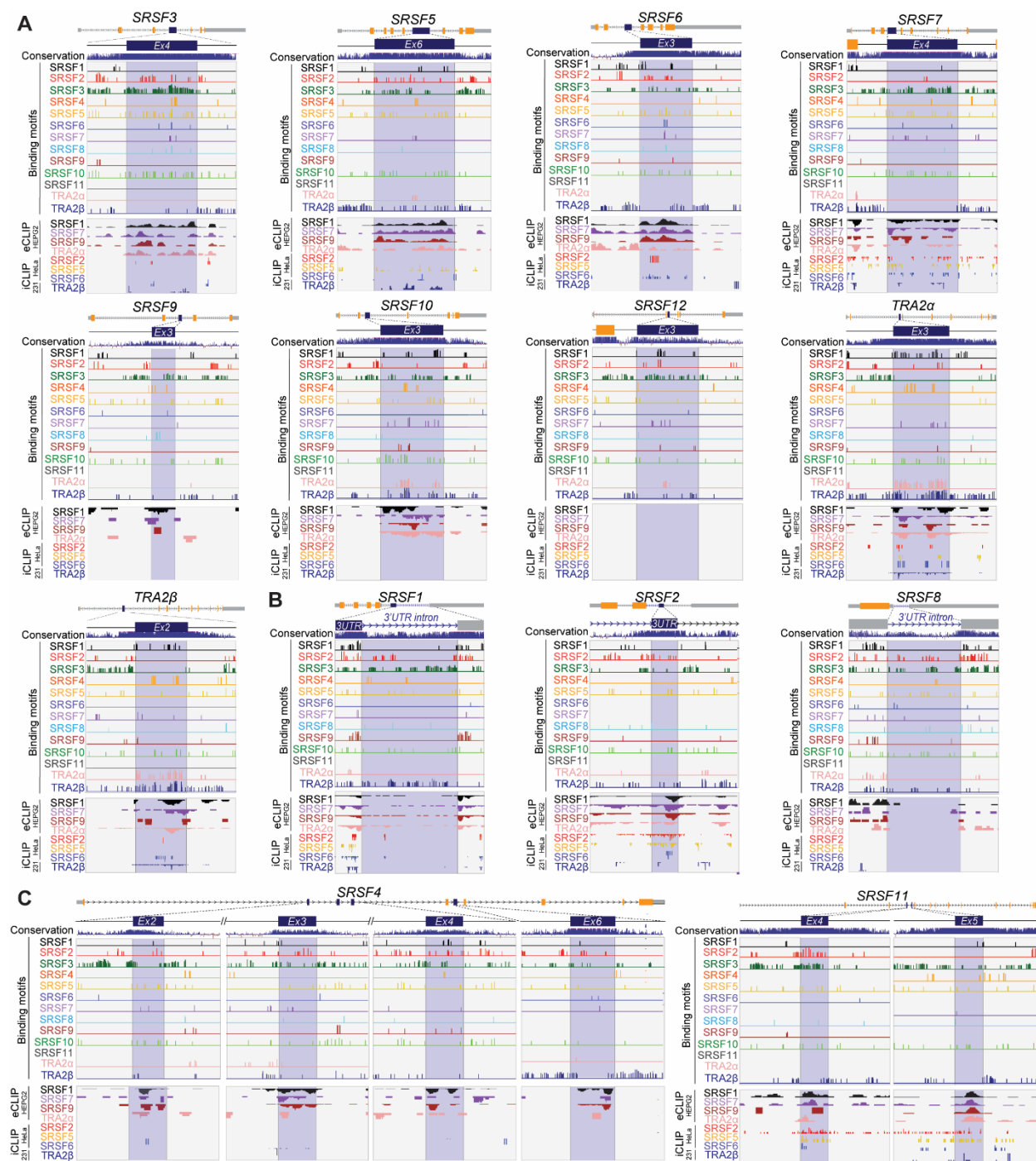


Figure S3. SR protein poison exon sequences contain binding sites for their other protein family members (related to Figure 2).

(A) Predicted SR protein RNA binding motifs and experimental support for binding to *SR-PE* sequences. Schematic of SR protein gene structures 5' to 3' with internal single cassette poison exons (not at scale), along with the evolutionary conservation across 100 vertebrates (top panel). Zoomed in regions shows the location of ultraconserved regions with binding motifs from RBPmap (middle panel) and CLIP-seq read coverage (bottom panel) within the poison exon or poison

sequence (blue). See [Table S2](#) for RBP RNA binding motifs. CLIP-seq data from HepG2 and K562 cells (ENCODE datasets), as well as HeLa and MDA-MB231 (Best et al., 2014; Krchnakova et al., 2019; Van Nostrand et al., 2016).

(B,C) Same as in **(A)** for SR proteins with 3'UTR poison sequences (B) or with multiple PEs (C).

Figure S4

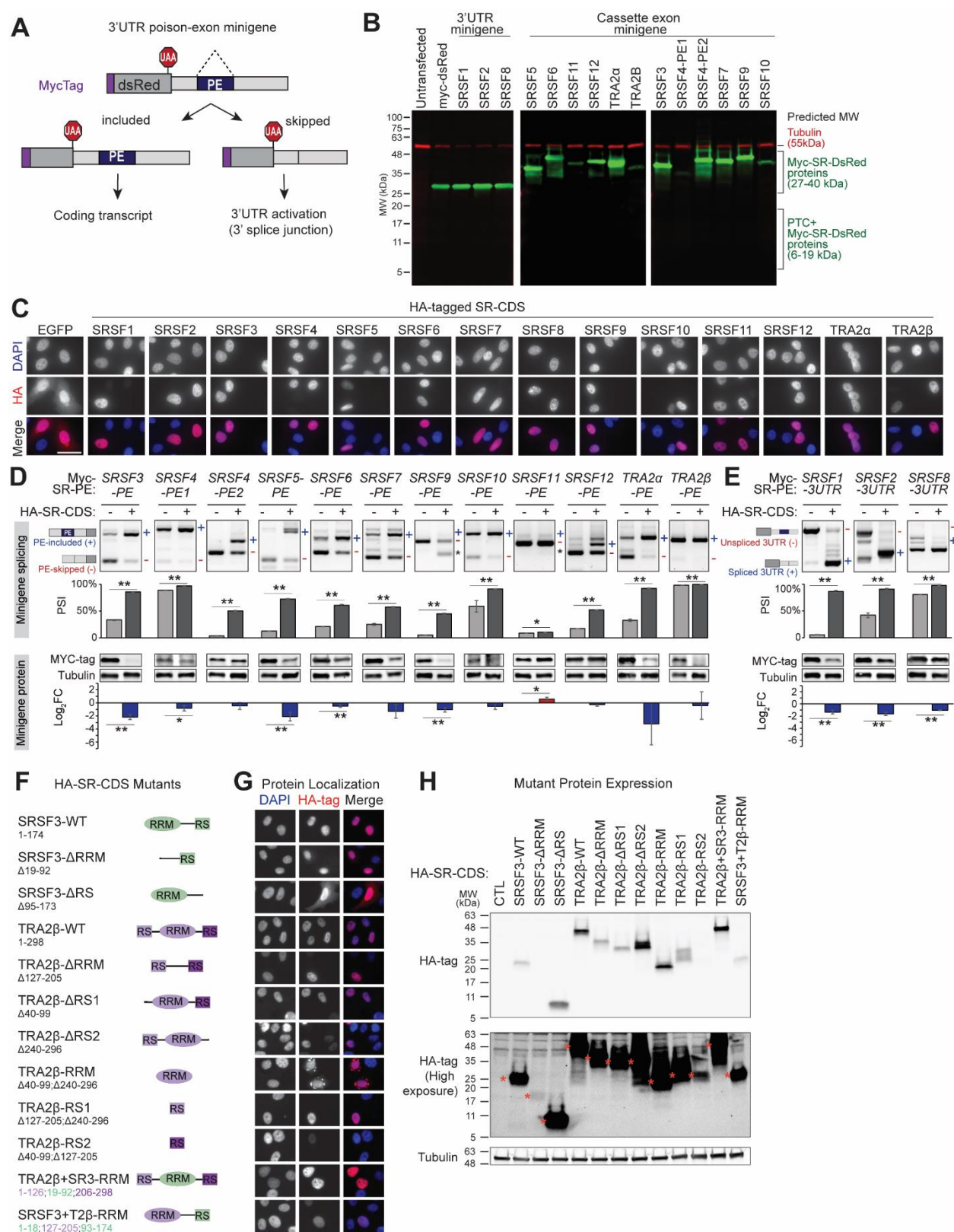


Figure S4. SR proteins use poison exons to auto- and cross-regulate their protein expression (related to Figures 2 and 4).

(A) Schematic of the splicing reporter minigene for 3'UTR poison sequences and resulting processed isoforms. Sequences encoding the Myc-epitope tag, dsRed protein, and stop codon locations are indicated. For *SRSF1* and *SRSF8*, removal of 3'UTR introns results in formation of a splice junction after the canonical stop codon. For *SRSF2*, the AS-NMD transcript requires removal of 3'UTR introns as well as inclusion of a 3'UTR exon.

(B) Representative western blot analysis of Myc-tagged proteins expressed from *SR-PE* minigenes in HEK293 cells using a minigene specific Myc-tag antibody (green) and tubulin (red) as a loading control. Minigenes are grouped by 3'UTR or cassette exons presence, as well as based on protein expression for cassette exon minigenes. SR protein minigenes produce one discrete band on western blot with no detectable truncated products from potential translation of premature termination codon (PTC+)-containing transcripts. All three SR protein 3'UTR minigenes produce a 27kDa Myc-tagged Ds-Red-containing protein, whereas cassette exon minigenes produce Myc-tagged Ds-Red-containing proteins ranging in predicted molecular weight (MW) between 27-45kDa.

(C) Representative immunofluorescence images of HeLa cells transfected with HA-CDS-SR expression plasmids, stained with mouse anti-HA antibody and Alexa568 secondary antibody. Nuclei are counterstained with DAPI (scale, 30µm).

(D) PE splicing and protein expression from HEK293 cells co-transfected with cassette PE minigenes along with HA-CDS-SR plasmid for the corresponding SR protein or empty vector control. Exon inclusion is quantified using RT-PCR with minigene specific primers that amplifies both exon skipping and included isoforms. Increased exon inclusion ($\Delta\text{PSI} > 0$) or skipping ($\Delta\text{PSI} < 0$) is relative to empty vector control ($n=3$, mean \pm sd; t-test, $*P < 0.05$, $**P < 0.01$). Log₂ Fold change (Log₂FC) protein expression is quantified by western blot using a minigene specific Myc-tag antibody and tubulin as a loading control, normalized to empty vector control ($n=3$, mean \pm sd; t-test, $*P < 0.05$, $**P < 0.01$).

Novel examples of validated autoregulation include: *SRSF4* which contains two sets of PEs, either exons 2, 3 and 4 which are included together (*SRSF4-PE1*) or exon 6 alone (*SRSF4-PE2*). Previous studies have shown that exogenous *SRSF4* expression can decrease the endogenous protein expression and that *SRSF4* directly binds to its PEs through CLIP-seq, but have not shown this interaction to be directly attributed to splicing of its PE (Anko et al., 2010; Anko et al., 2012).

Additionally, we identify autoregulation of PE inclusion in *SRSF6*, *SRSF10*, *SRSF12*, and *TRA2 α* , and of 3'UTR poison sequences in *SRSF8*. Notably, the *SRSF9* and *SRSF11* minigenes undergo alternative splicing to create transcripts that contain a frameshift due to skipping of both the PE and adjacent downstream exon (denoted with an asterisk *). This creates a frameshift and premature termination codon (PTC) in the *SRSF9-PE* minigene but not in the *SRSF11-PE*. However, both of these splicing events lead to frameshift-induced PTCs in the endogenous gene.

The *SRSF12-PE* minigene contains five total exons to recapitulate the minor and major spliceosome sites across these exons in the endogenous context. Splicing of *SRSF12-PE* leads to 3 distinct isoforms detected by PCR: i) the top band contains the PE and next downstream exon that utilizes an alternative 3'SS corresponding to the major spliceosome; ii) the middle band contains the PE and skips the next downstream exon; iii) the bottom band skips the PE and contains all of the coding sequence exons. The top and middle bands are included for quantification of *PE* PSI.

(E) Same as in **(D)** for SR protein 3'UTR minigenes. AS-NMD events in the UTR of *SRSF1*, *SRSF2*, and *SRSF8* are more complex than those of cassette PEs. For *SRSF1*, alternative splicing of the 3'UTR involves multiple intron removals that flank ultraconserved regions and

multiple splicing events can be induced by SRSF1 overexpression and stabilized by NMD inhibition (Lareau et al., 2007; Sun et al., 2010). We confirmed our SRSF1-3UTR minigene recapitulates its reported autoregulatory splicing through sanger sequencing, however the minigene uses a 5' splice site (5'SS) located 14bp downstream of the 3'UTR 5'SS sequence and 4bp into the dsRed sequence, and which is predicted to have similar strength as the endogenous 5'SS. The SRSF2-3UTR minigene autoregulation utilized inclusion of an exonic sequence within the 3'UTR as described for the endogenous gene (Lareau et al., 2007; Sureau et al., 2001).

(F) Domain structure of wild-type and mutant SRSF3 and TRA2 β proteins. Included or deleted (Δ) amino acids positions are indicated. RRM: RNA-recognition motif; RS: arginine-serine rich domain.

(G) Representative immunofluorescence images of HeLa cells transfected with 500ng of HA-CDS-SR expression plasmids from (A), stained with mouse anti-HA antibody and Alexa568 secondary antibody. Nuclei are counterstained with DAPI (scale, 30um).

(H) Expression of HA-CDS-SR expression plasmids from (A) in HeLa cells detected by western blotting with anti-HA antibody and tubulin as a loading control. Bands corresponding to the expected protein molecular weight (MW) are marked with orange asterisk (*).

Figure S5

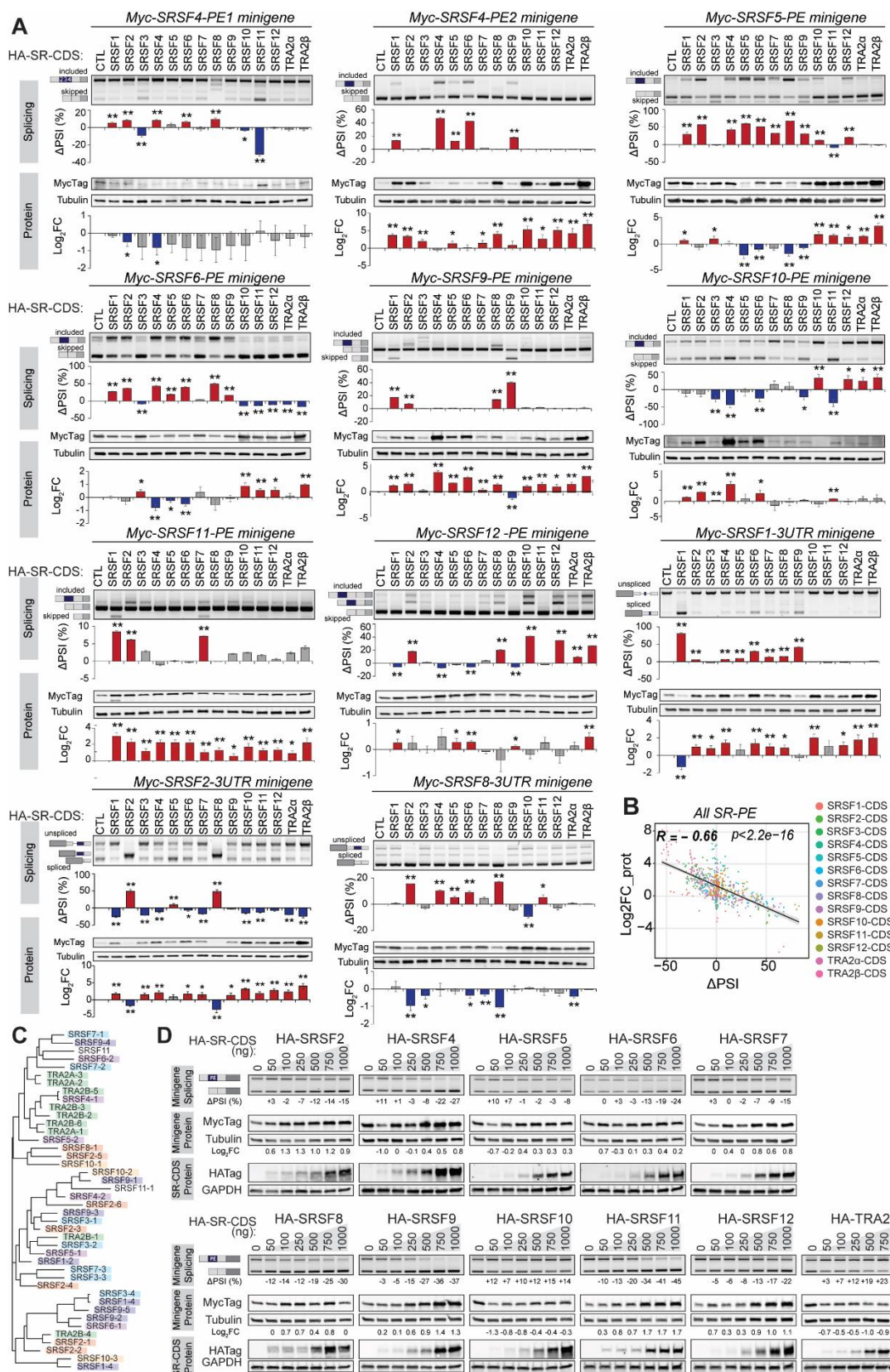


Figure S5. SR proteins cross-regulate their expression in a dose-dependent manner through alternative splicing of poison exons (related to Figure 2-3).

(A) PE splicing and protein expression is measured by semi-quantitative RT-PCR using minigene specific primers that amplify both the included and skipped isoforms. Increased exon inclusion ($\Delta\text{PSI}>0$) or skipping ($\Delta\text{PSI}<0$) is relative to empty vector control ($n=3$, mean \pm sd; t-test, $*P<0.05$, $**P<0.01$). Log_2 Fold change (Log_2FC) protein expression is quantified by western blot using a minigene specific Myc-tag antibody and tubulin as a loading control, normalized to empty vector control ($n=3$, mean \pm sd; t-test, $*P<0.05$, $**P<0.01$).

(B) Pearson correlation between SR protein minigene splicing (ΔPSI) and SR protein expression (Log_2FC) aggregated for all SR-PEs in cells transfected with indicated SR-CDS, as quantified in [Figures 2C-F](#) and [S5A](#). P -values are indicated. See also [Table S3](#).

(C) Clustering of SR protein motifs based on sequence similarity. Related SR protein family members are similarly colored.

(D) PE splicing and protein expression from the *TRA2 β -PE* minigene in HeLa cells cotransfected with and increasing concentration of indicated HA-SR-CDS plasmids (supplemented up to 1000ng of DNA with control empty vector). *TRA2 β -PE* inclusion is measured by semi-quantitative RT-PCR using minigene specific primers that amplify both the included and skipped isoforms. Increased exon inclusion ($\Delta\text{PSI}>0$) or skipping ($\Delta\text{PSI}<0$) is relative to empty vector control. Log_2 Fold change (Log_2FC) protein expression is quantified by western blotting using a minigene specific Myc-tag antibody and tubulin as a loading control, normalized to empty vector control. HA-SR-CDS protein expression is detected using HA-tag antibody and GAPDH as a loading control. See also heatmap representation of PE splicing and protein levels in [Figure 3B](#).

Figure S6

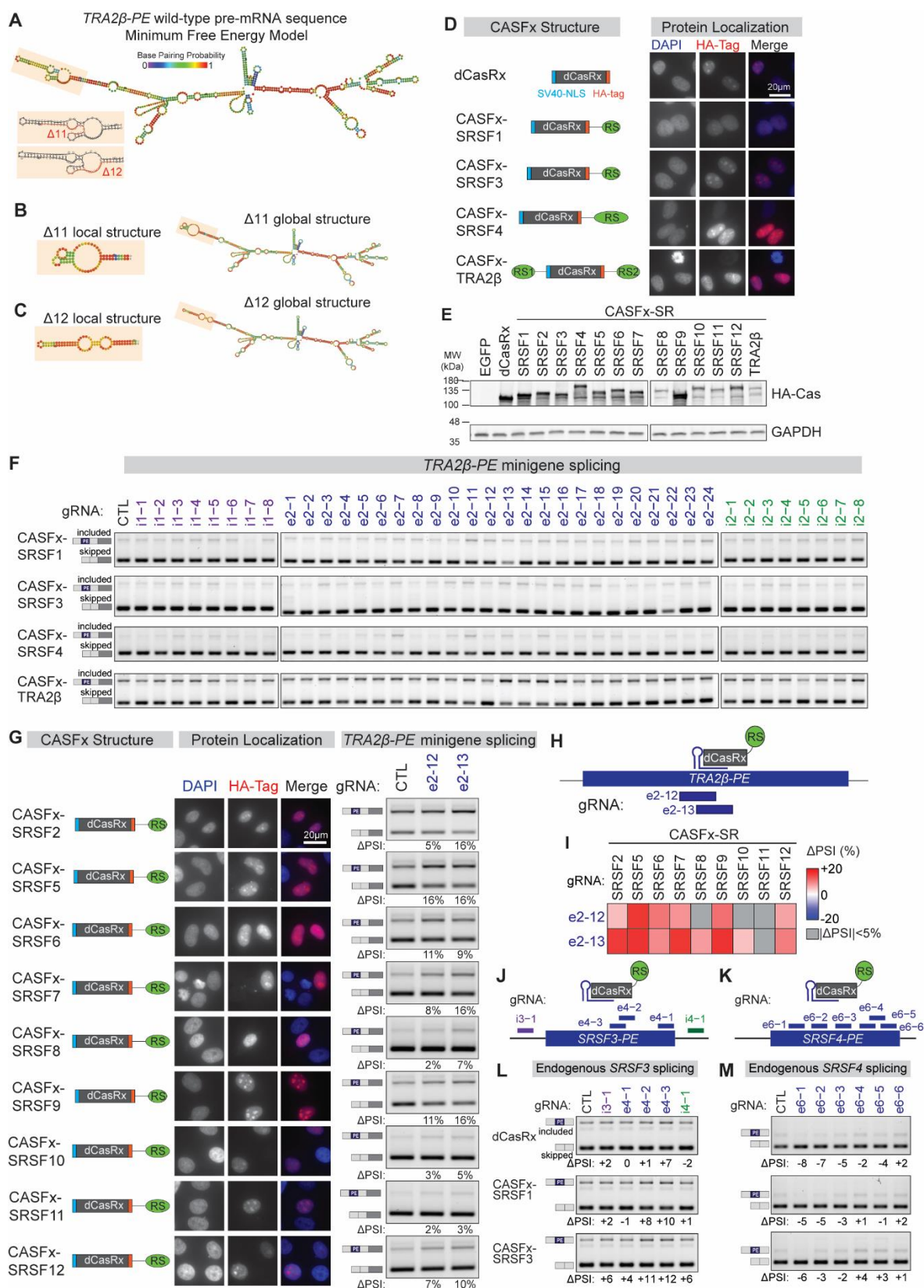


Figure S6. Defining the splicing regulatory elements and splicing regulators of *TRA2β-PE* inclusion (related to Figures 5, 6).

(A) Predicted minimum free energy structure of wild-type *TRA2β-PE* and 250bp of flanking intron sequences using RNA fold (<http://rna.tbi.univie.ac.at/cgi-bin/RNAWebSuite/RNAfold.cgi>) (Lorenz et al., 2011). The *TRA2β-PE* Δ11 and Δ12 region is highlighted.

(B-C) Predicted minimum free energy structure of *TRA2β-PE* and 250bp of flanking intron for the *TRA2β-PE* Δ11 (**B**) and Δ12 (**C**) deletion mutants.

(D) Structure and localization of HA-tagged CASFx-SR proteins. Diagrams indicating CASFx-SR protein structures consisting of N-terminal dCasRx and C-terminal RS domain for each SR protein (SRSF1-12), or N-terminal RS1 domain followed by dCasRx and C-terminal RS2 domain for *TRA2β*. Representative immunofluorescence images of HeLa cells transfected with 500ng of CASFx-SR proteins plasmids, stained with mouse anti-HA antibody and Alexa-568 secondary antibody. Nuclei are counterstained with DAPI (scale, 20μm).

(E) Protein expression HA-tagged CASFx-SR proteins transfected in HEK293T cells is assessed at 48h post transfection by western blotting with an HA-tag antibody and tubulin as a loading control.

(F) *TRA2β-PE* inclusion is assessed using RT-PCR with minigene specific primers and normalized as ΔPSI to non-targeting control gRNA (CTL) as summarized in the heatmap [Figure 6C](#).

(G) Structure and localization of additional CASFx-SR proteins as in **(D)** *TRA2β-PE* splicing assessed by cotransfecting HEK293T cells with the *TRA2β-PE* minigene, CASFx-SR protein plasmid, and indicated gRNA plasmid. *TRA2β-PE* inclusion is measured by semi-quantitative RT-PCR using minigene specific primers that amplify both the included and skipped isoforms, and normalized to non-targeting control gRNA (CTL). Binding positions of the 22nt gRNAs targeting the *TRA2β* poison exon (e2-12 and e2-13) are indicated (**E**).

(H) Target sites for 22nt gRNAs in dCasRx and CASFx-SR proteins in *SRSF3-PE* and flanking introns.

(I) Heatmap representation of *TRA2β-PE* splicing from **(D)** as ΔPSI for each targeting gRNA vs. non-targeting control gRNA (CTL).

(J,L) PE inclusion in the endogenous *SRSF3* transcript is measured in HEK293T cells transfected with indicated dCasRx or CASFx-SR plasmids and gRNAs targeting *SRSF3-PE* or surrounding introns. *SRSF3-PE* inclusion assessed using RT-PCR with gene specific primers and normalized as ΔPSI to non-targeting control gRNA (CTL).

(K,M) Same as in **(J,L)** with the endogenous *SRSF4* transcript.

Figure S7

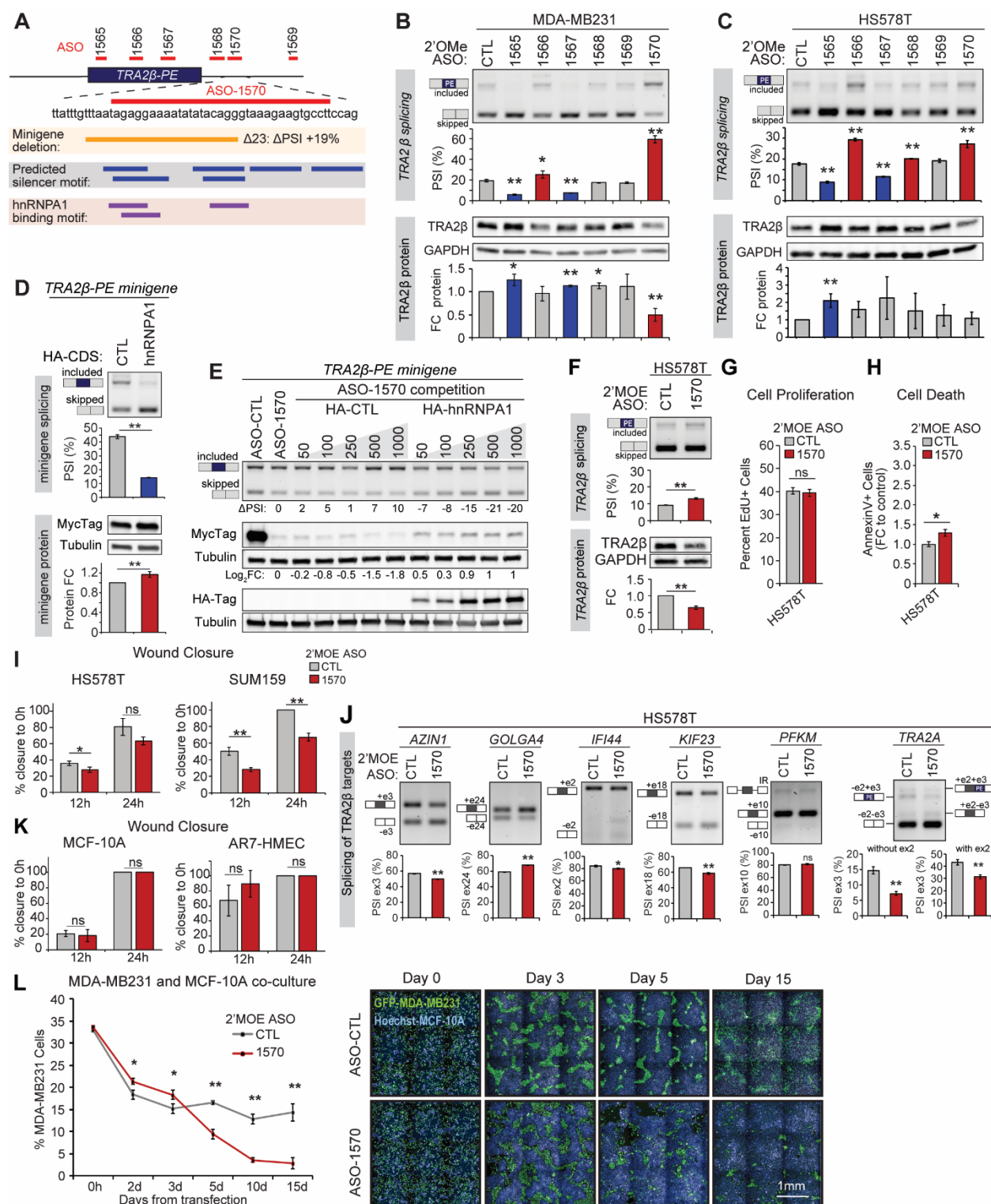


Figure S7. *TRA2β*-targeting ASOs impact *TRA2β*-PE splicing as well as *TRA2β* protein expression and activity (related to Figure 7).

(A) Binding locations of ASOs targeting *TRA2β*-PE and the downstream intron. The bottom panel shows the binding sequence of ASO-1570 along with the location of $\Delta 23$ deletion from Figure 5, as well as splicing silencer and HNRNPA1 binding motifs predicted by Human Splicing Finder (Desmet et al., 2009).

(B-C) *TRA2β*-PE splicing in MDA-MB231 **(B)** and HS578T **(C)** cells transfected with 50nM of *TRA2β*-targeting or non-targeting control (CTL) 2'-O-methyl-phosphorothioated (2'OMe) ASOs. *TRA2β*-PE inclusion and *TRA2β* protein expression are measured with RT-PCR and western blot, respectively, 48h after transfection (n=3, mean \pm SD; t-test, * P <0.05, ** P <0.01).

(D) HeLa cells cotransfected with the *TRA2β*-PE minigene and either a control plasmid (CTL) or one encoding an HA-tagged hnRNPA1-CDS. Minigene splicing and protein production assessed by RT-PCR and western blotting 48h after transfection (n=3, mean \pm SD; t-test, * P <0.05, ** P <0.01).

(E) HeLa cells cotransfected with the *TRA2β*-PE minigene along with *TRA2β*-targeting (1570) or control (CTL) ASO alone, or with increasing amounts of HA-hnRNPA1-CDS or control plasmids. Minigene splicing and protein production assessed by RT-PCR and western blotting 48h after transfection, compared to ASO-1570 alone.

(F) *TRA2β*-PE splicing and *TRA2β* protein expression in HS578T cells transfected with 50nM of ASO-1570 (n=3, mean \pm SD; t-test, * P <0.05, ** P <0.01).

(G) Cell proliferation in HS578T breast cancer cells transfected with 50nM of 2'MOE ASO-1570 vs. -CTL is quantified by 5-Ethynyl-2'-deoxyuridine (EdU) incorporation 48h after transfection. Representative stains for Alexa 647 EdU and Hoechst in MDA-MB231 cells are shown in the left panel. The percent of EdU+ cells to total Hoechst+ cells is shown (n=3, mean \pm SD; t-test, * P <0.05, ** P <0.01).

(H) Cell death in HS578T breast cancer cells transfected with 50nM of 2'MOE ASO-1570 vs. -CTL is quantified by AnnexinV staining 48h after transfection. Representative stains for Alexa 647 conjugated AnnexinV and Hoechst in MDA-MB231 and SUM159 cells are shown in the left panel. The percent of AnnexinV+ cells to total Hoechst+ cells is normalized to ASO-CTL (n=3, mean \pm SD; t-test, * P <0.05, ** P <0.01).

(I) Wound closure assays in HS578T and SUM159 cells transfected with 50nM of 2'MOE ASO-1570 vs. -CTL. Percent wound closure is relative to 0h (n=3, mean \pm SD; t-test, * P <0.05, ** P <0.01).

(J) Splicing of known *TRA2β* target transcripts is measured in HS578T cells transfected with 50nM of 2'-O-methoxyethyl-phosphorothioated (2'MOE) ASO-1570 vs. -CTL, 48h after ASO transfection. Exon inclusion is measured by RT-PCR (n=3, mean \pm SD; t-test * P <0.05, ** P <0.01).

(K) Wound closure assays in MCF-10A and AR7-HMEC non-transformed mammary epithelial cells transfected with 50nM of 2'MOE ASO-1570 vs. -CTL. Percent wound closure is relative to 0h (n=3, mean \pm SD; t-test, * P <0.05, ** P <0.01).

(L) GFP-tagged MDA-MB231 co-cultured with MCF-10A cells are transfected with 50nM of 2'MOE ASO-1570 vs. -CTL. Cell number is quantified at various timepoints by live cell imaging with GFP and Hoechst stain. The proportion of MDA-MB231 cells is calculated as number of GFP+ cells divided by total number of Hoechst+ nuclei (n=3, mean \pm SD; t-test, * P <0.05, ** P <0.01).